論文の内容の要旨

Evolution and nucleosynthesis of massive first stars

（大質量初代星の進化と元素合成）

氏名　髙橋 亘

First stars, also known as Population III (Pop III) stars, were key drivers of the evolution of the early universe. Their high energy radiations constituted an important component of ionizing photons to initiate the cosmic re-ionization. They were the first nuclear reactors in the chemically primitive universe, creating heavier isotopes than ^{7}Li. Massive first stars, furthermore, would explode as first supernovae in the universe. The explosions spread over the circumference, crushing and heating up the ambient gases. Processed stellar materials were ejected by the explosions and mixed with the primordial gases, changing the chemical properties.

In this thesis, I purpose to constrain the properties of first stars, such as the initial masses and the rotational properties, by conducting the *abundance profiling*. The key idea is that chemically primitive abundances observed from metal-poor stars in the local universe may preserve nucleosynthetic signatures occurred in the early universe. Assuming in this way, I try to make a link between the theoretically calculated yields of first supernovae in the early universe and the observationally collected abundances of metal-poor stars in the local universe. Demand for this kind of constraint has been increasing to examine theoretically estimated characteristics of first stars. Recent simulations estimate that first stars will show a wide initial mass function of ∼10–1000 $M_\odot$. Besides, first stars are suggested to have a fast rotation velocity at birth.

In order to infer progenitor's properties from abundance comparisons, one needs to know how characteristic chemical signatures are resulted from the specific progenitor in advance. Therefore, to begin with, I aim to find such characteristic nucleosynthesis patterns for Pop III core-collapse supernova (CCSN) yields in Chapter 3. Firstly, I conduct evolution calculations of 12–140 $M_\odot$ progenitors, with and without taking

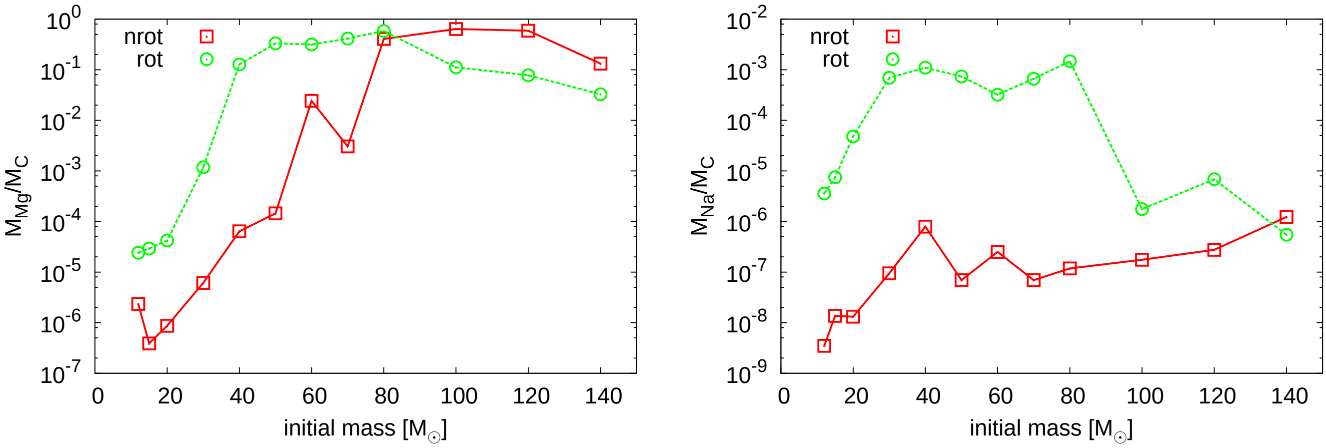

図 1: The production ratio, M_X/M_C, as a function of initial mass for magnesium (left) and for sodium (right). All isotopes distributing outer than the CO core are integrated. Red open squares show non-rotating results, and green open circles with dashed lines show rotating results, respectively.

the effects of rotation into account. Then the supernova yields are calculated by applying a simple but pragmatic model of the *weak explosion* model, which will provide suitable stellar yields for CEMP stars. The explosion is assumed to be too weak to affect the outer chemical distributions of the star, and only the weakly bound outer materials are ejected by the explosion.

I find that various abundance distributions arise in outer shell helium regions in calculated models. Massive models of $\geq$ 40 $M_\odot$ for rotating and $\geq$ 60–80 $M_\odot$ for non-rotating cases show both magnesium and silicon enhancement in their helium layers (Fig. 1, left panel). These enhancements are due to efficient alpha capture reactions in the region. As for rotating models, owing to rotationally induced mixing, abundant nitrogen is produced in the hydrogen burning shell at first. Alpha capture reactions onto nitrogen take place in later evolutionary phases, resulting in neutron emission and nucleosynthesis of sodium and aluminum (Fig. 1, right panel). For non-rotating heavy massive stars of $\geq$ 80 $M_\odot$, calcium production occurs in the hydrogen burning shell owing to break-out of the CNO cycle. These characteristics are well reflected in the stellar yields. The new findings will be useful to deduce the properties of source stars, which existed in the early universe.

In the next Chapter 4, a systematic calculation of pair-instability supernova (PISN) explosions and nucleosynthesis is conducted. I discuss in detail how energetics of PISN explosions can be treated in a simulation to accurately determine the initial mass range for PISNe, and I confirm that more massive 145–260 $M_\odot$ stars explode as PISNe. Then, in order to determine characteristic abundance patterns that can be used to distinguish the PISN yields from the other, the explosive yield is calculated based on the explosion simulation using the exact formulation of the energy conservation.

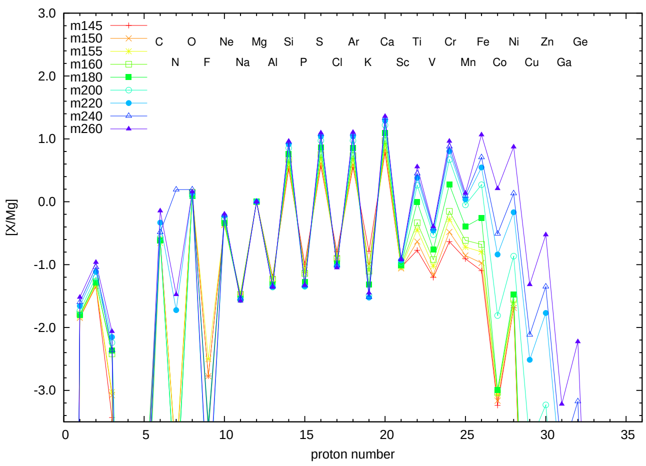

図 2: Abundance patterns of PISN yields. The abundance of magnesium is used for the normalization.

First, the pronounced odd-even variance is confirmed in my calculation (Fig. 2). Furthermore, I find that the elemental yield can be divided into three groups based on the mass dependencies. First group consists of lighter elements of carbon to aluminum. Their abundance pattern is almost constant with changing the initial mass of the star. In addition to the lighter elements, scandium shows similar constancy. Therefore, abundance ratios such as [Na/Mg], [Al/Mg], and [Sc/Mg] can be used as the first requirement for a hypothetical PISN child to exhibit. Deficiencies of them can be interpreted as realization of the odd-even variance. The second group, the intermediate-mass elements from silicon to calcium, is composed of products of oxygen burning. The odd-even variance in these elements is found to show the initial mass dependence. Thus the abundance patterns such as [Si/Mg] and [Ca/Mg] can be used as a potential probe to constrain the initial mass of the PISN source star. Finally, the heaviest elements from titanium to germanium show the strongest mass dependence. The steep decline around the proton number of 28–32, which can be indicated by abundance ratios of [Ni/Fe] or [Zn/Ni], can be used as the second requirement to search PISN children.

Eventually, I conduct abundance comparisons between the theoretical yields and observations, in Chapter 5. As a demonstration of the weak supernova model, I compare the theoretical yields with the three most-iron-poor stars discovered so far, to constrain the initial masses and rotational properties of source stars of the metal pollution. They are SMSS 0313-6708 of [Fe/H] < -7.1 (Keller et al. 2014), HE 0107-5240 of [Fe/H] $= -5.3$ (Christlieb et al. 2002), and HE 1327-2326 of [Fe/H] $= -5.7$ (Frebel et al. 2005). All of these stars are member of CEMP stars, having a large carbon abundance compared to iron of [C/Fe] > 0.7. Moreover, they are also known to show enhancements in intermediate-mass elements, such as sodium, magnesium, and silicon. Therefore it is expected that a weak supernova model, which abundantly produces such intermediate-mass elements synthesized in the outer region of the progenitor, can provide a reasonable fitting.

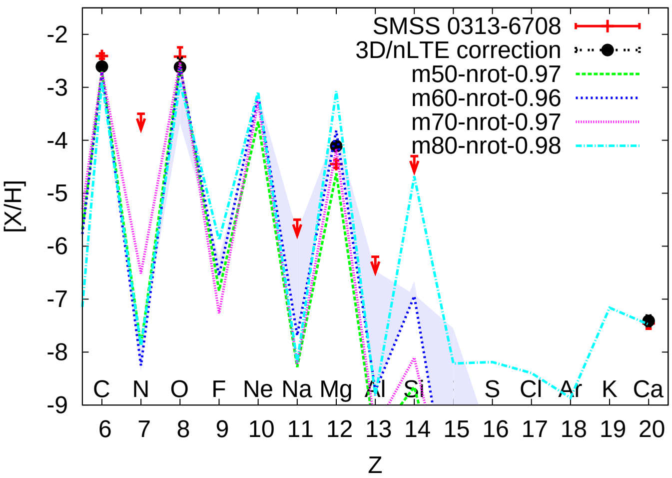

図 3: The abundance pattern of SMSS 0313-6708. Red crosses and arrows show observed values and upper limits, and black points show corrected values accounting for the effect of 3D/non-LTE stellar atmosphere, respectively. The best-fit non-rotating 60 $M_\odot$ model is shown by the blue-dotted line.

The abundance pattern of SMSS 0313-6708 can be explained by non-rotating massive 50–80 $M_\odot$ models with large inner boundaries of ejections, $f_{\rm ej} \sim 0.92$–1.00, where $f_{\rm ej} \equiv M_{\rm ej}/M_{\rm CO}$ is a non-dimensional parameter showing the position of the ejection by comparing to the CO core mass (Fig. 3). The non-rotating 60 $M_\odot$ model provides the best explanation for both the observed low [Mg/C] and the upper limits on [Na, Al/C], while the low abundance of [Ca/C] can be consistently explained by the 80 $M_\odot$ model. The reliability of the model is further reinforced by recent observational confirmation of the high oxygen abundance of [O/C] ~ 0. Abundances of [N, O, Na/C] in HE 0107-5240 can be consistently explained by a rotating 30 $M_\odot$ model. The wide acceptable range in $f_{\rm ej} \sim 1.01$–1.13 suggests the robustness of this model. Moreover, 30 and 40 $M_\odot$ models with slower rotations provide much better fitting results for the sodium abundance. HE 1327-2326 has a small [O/C] and an interesting decreasing trend of [Na, Mg, Al/C]. These abundances are consistently explained by both rotating and non-rotating 15–40 $M_\odot$ models, ejecting the mass from the outer edge of the carbon burning regions, $f_{\rm ej} \sim 0.92$–0.97. To explain the large abundance of [N/C], much faster rotation or another origins than the single explosion may be needed.

Although a growing number of metal-poor stars have been discovered by recent observations, an yield comparison of PISN yields with observations has not been made except for the recent work by Aoki et al. (2014). This will be partly due to the comprehension that no candidates for the PISN children have been discovered from the EMP stellar samples. The reason of the non-detection can be explained as a

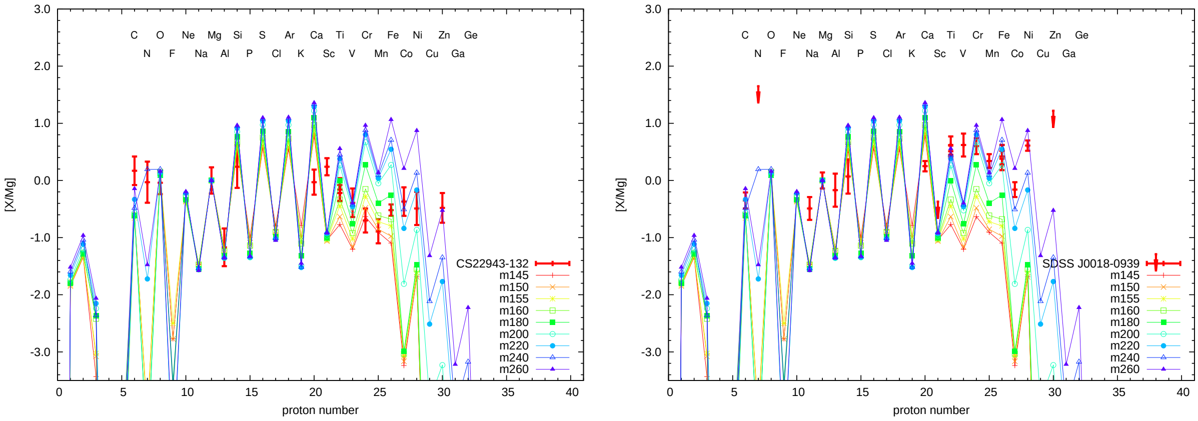

図 4: The abundance pattern of CS22943-132 (left) and SDSS J0018-0939 (Aoki et al. 2014, right). Red thick crosses show observed values, while PISN yields are shown by thin lines.

result of the observational bias. Because of the large metal yield, PISN children may be born having a relatively large [Ca/H] ~ -2.5, which can be missed from metal-poor star huntings utilizing the CaII K line. Therefore I have conducted the first systematic comparison between the theoretical PISN yields and large numbers of surface abundances of metal-poor stars compiled in *SAGA* database. The purpose of this comparison is to find candidates of PISN children and to validate the applicability of characteristic abundance patterns proposed in Chapter 4.

Unfortunately, I have found no candidate metal-poor stars included in the sample that exhibit characteristic abundance signatures of PISN yields. For example, abundance ratio of CS22943-132 is shown in the left panel of Fig. 4. First, the predicted [Na/Mg] $= -1.58 - -1.46$ is too low to be compared with the current stellar observations, and second, the high [Ca/Mg] $= 0.78 - 1.35$ exclude most of the metal-poor stars out from the candidates of PISN children. However, by making the direct comparisons, effectiveness of theoretically proposed abundance patterns can be verified. In addition to the [Na/Mg] ratio, the [Sc/Mg] ratio is found to be useful as the indicator of the odd-even variance of the PISN yields. Also, the low [Zn/Mg] < -0.52 due to the low explosion temperature can be used as a firm requirement for the candidate abundance pattern. The abundance pattern observed in the iron-peak elements, in most cases, is found to give critical inconsistency to the model yields: the small initial mass suggested by [Cr/Mg] is in complete disagreement with the large initial mass obtained by [Co/Mg], if the metal-poor star has a typical value of [Cr/Co] < 0. The interesting example, SDSS J0018-0909, has the exceptionally small [Co/Mg] ratio as discussed in Aoki et al. 2014, however, the large odd-Z abundances of [Na, Al, V/Mg] and the small [Ca/Mg] are inconsistent with PISN yields (Fig. 4, right panel).

Abundance profiling enables us to investigate the characteristics of massive first stars existed in the far-away early universe. By the comparison with the most-iron-deficient stars, indication of the existence of $\sim$ 15–80 $M_\odot$ first stars is obtained for the first time. Some of them would rotate, but some of others would not. Further investigation will provide invaluable information on the properties of massive first stars. On the other hand, the characteristic yields of $\sim$ 100–140 $M_\odot$ stars, large abundance ratios of [O/C] and [Mg, Si/C], have not been found from the HMP stars. Moreover, no signature of PISN yields occurring from 145–260 $M_\odot$ first stars has been found from the current big sample of metal-poor stellar abundances. These result are incompatible with the wide initial mass distribution of first stars estimated by the recent cosmological simulations. Where are children of very massive first stars? This remains as a big open question in investigations of the early universe.